Journal of Power Sources 195 (2010) 4308–4312

Contents lists available at ScienceDirect

Journal of Power Sources

journal homepage: www.elsevier.com/locate/jpowsour

Short communication

Preparation and characterization of Na-doped $LiFePO_4$/C composites as cathode materials for lithium-ion batteries

Xiongge Yin, Kelong Huang*, Suqin Liu, Haiyan Wang, Hao Wang

College of Chemistry and Chemical Engineering, Central South University, Changsha 410083, Hunan, China

ARTICLE INFO

Article history:
Received 12 November 2009
Received in revised form 4 January 2010
Accepted 8 January 2010
Available online 15 January 2010

Keywords:
$LiFePO_4$
Na doping
In situ polymerization restriction
Lithium-ion batteries

ABSTRACT

To improve the performance of $LiFePO_4$, single phase $Li_{1-x}Na_xFePO_4$/C ($x = 0$, 0.01, 0.03, 0.05) samples are synthesized by in situ polymerization restriction–carbonthermal reduction method. The effects of Na doping are studied by X-ray diffraction (XRD), scanning electron microscopy (SEM), transmission electron microscope (TEM), cyclic voltammetry (CV) and electrochemical impedance spectroscopy (EIS). The results indicate that doped Na ion does not destroy the lattice structure of $LiFePO_4$, while enlarges the lattice volume. Electrochemical test results show that the $Li_{0.97}Na_{0.03}FePO_4$/C sample exhibits the best electrochemical performance with initial special discharge capacity of 158 mAh g^{-1} at 0.1 C. EIS results demonstrate that the charge transfer resistance of the sample decreases greatly by doping an appropriate amount of Na.

1. Introduction

Olivine-type $LiFePO_4$ is considered to be one of the most promising cathode materials for the next generation of lithium-ion batteries due to its low toxicity, low cost, and high safety [1,2]. However, its power performance is greatly limited by slow diffusion of lithium ions across the two-phase boundary and its low electronic conductivity [3,4].

Effective approaches have been introduced to improve the poor rate performance of $LiFePO_4$, including coating $LiFePO_4$ particles with electrically conductive materials like carbon [5], metal and metal oxides [6–8], minimizing the particle size [9,10] and doping with supervalent cations [11]. However, the performance of the high valence metal ion doped material was not improved as expected. It was found that $LiFePO_4$ possessed one-dimensional lithium ion diffusion pathway [12,13], and the doped high valence transition metal ions at the Li site in $LiFePO_4$ would block the one-dimensional diffusion pathway, which resulted in lower ionic conductivity [14]. Ouyang et al. [15] have investigated the electronic structure and ionic dynamic properties of pure and Na-doped (Li site) $LiFePO_4$ by the first-principles calculations. The calculated results showed that not only the electronic conductive properties were enhanced by Na doping, but also the ionic transport feature was favourable for high rate performance, compared with the high valance metal ions doping (such as Cr) and pure $LiFePO_4$. Therefore, in this paper, we experimentally investigated the effects of Na doping on the electrochemical properties of $LiFePO_4$/C cathode material.

In order to improve the conductivity of the solid phase by reducing the particle size and creating conductive carbon coatings, we adopt an in situ polymerization restriction–carbonthermal reduction method for the synthesis of the $LiFePO_4$/carbon composites [16]. The $FePO_4$/polyaniline (PANI) precursor was prepared by in situ polymerization reaction to restrict the growth of the $FePO_4$ particle. Subsequent heat treatment at 700 °C under argon in the presence of lithium salt, sodium salt and some glucose led to the transformation of this $FePO_4$/PANI composite into a $Li_{1-x}Na_xFePO_4$/C composite ($0 \le x \le 0.05$). Then the physical and electrochemical properties of the prepared powders were investigated.

2. Experimental

The starting materials for synthesizing the $FePO_4$/PANI composite were $Fe(NO_3)_3 \cdot 9H_2O$, $NH_4H_2PO_4$, and aniline. In a typical experiment, 100 mL of solution containing 0.025 mol $Fe(NO_3)_3 \cdot 9H_2O$ was slowly added, with stirring, to 200 mL of solution containing 0.025 mol $NH_4H_2PO_4$ and 1 mL of aniline. The pH of the solution was adjusted to 2.1 by adding ammonia. The reaction mixture was then stirred for 8 h at room temperature and the resulting $FePO_4$/PANI composite was filtered and washed several times with distilled water and ethanol successively. The $Li_{1-x}Na_xFePO_4$/C ($x = 0$, 0.01, 0.03, 0.05) composites were synthesized from the prepared $FePO_4$/PANI composite by mixing with an equimolar amount

* Corresponding author. Tel.: +86 731 8887 9850; fax: +86 731 8887 9850.
E-mail address: huangkelong@163.com (K. Huang).

0378-7753/$ – see front matter © 2010 Elsevier B.V. All rights reserved.
doi:10.1016/j.jpowsour.2010.01.019

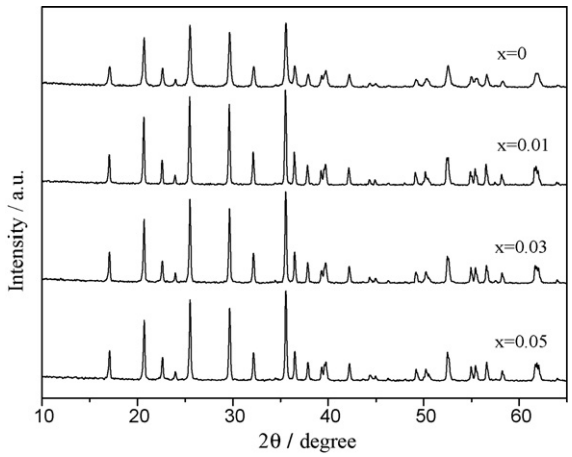

Fig. 1. XRD patterns of $Li_{1-x}Na_xFePO_4/C$ ($0 \le x \le 0.05$).

of CH_3COOLi (with respect to the amount of $FePO_4$ in the prepared composite), a certain amount of $NaNO_3$ and some glucose. After mixing uniformly, the precursors were heated at 350 °C for 5 h under argon. The mixture was then milled for 5 h and finally calcined at 700 °C for 10 h under argon to obtain the $LiFePO_4/C$ composite.

X-ray diffraction of the product was carried on a RigaKu D/max2550VB$^+$ 18 kW using graphite-monochromatized Cu Kα radiation (40 kV, 250 mA). The morphology of the as-prepared $LiFePO_4$ powder was observed by a JEM-2010 transmission electron microscope (TEM) and a JSM-6360-LV scanning electron microscopy (SEM) equipped with an energy dispersive spectrometer (EDS), respectively. The content of carbon was determined by C-S 800 infrared carbon sulphur analyzer. Electronic conductivity measurements were carried out by four-point probe method using a RTS-9 Digital Instrument.

The composite cathodes were prepared by mixing the prepared powders with acetylene black, and polyvinylidene fluoride (PVDF) in the weight ratio of 80:10:10. The slurry was then coated onto a non-corrosive stainless steel current collector (Ø 9 mm) at 15 MPa and dried at 120 °C for 12 h in a vacuum oven. The CR2016 coin cells were assembled in an argon-filled glove box (Mbraun, Unilab, Germany) with a lithium foil as the counter electrode. The electrolyte was 1 M $LiPF_6$ in a mixture of EC–DMC–DEC (volume ratio of 1:1:1) electrolyte. The cells were galvanostatically charged and discharged between 2.5 and 4.2 V at 28 °C on the electrochemical test instrument (CT2001A, Wuhan Land Electronic Co. Ltd., China). Cyclic voltammetry measurements were performed using electrochemical workstation (Shanghai Chenhua Instrument Co. Ltd., China) at a scan rate of 0.1 mV s^{-1} between 2.5 and 4.2 V. Electrochemical impedance spectroscopy was performed with a

Table 1
Lattice parameters of $Li_{1-x}Na_xFePO_4/C$.

Sample	a (Å)	b (Å)	c (Å)	V (Å^3)
$LiFePO_4/C$	10.2923	6.0085	4.7126	291.4332
$Li_{0.99}Na_{0.01}FePO_4/C$	10.2945	6.0083	4.7159	291.6898
$Li_{0.97}Na_{0.03}FePO_4/C$	10.3219	6.0014	4.7239	292.6220
$Li_{0.95}Na_{0.05}FePO_4/C$	10.3003	6.0144	4.7208	292.4571

ZAHNER-IM6 electrochemical workstation (Germany). The sinusoidal excitation voltage applied to the cells was 5 mV with a frequency range of between 0.01 Hz and 100 kHz. All potentials are cited in this paper with respect to the reference Li^+/Li. In order to examine if the sodium ion was inserted and extracted during the charge–discharge process, the element of Na in the electrolyte extracted from the home-made cells was analyzed using a PS-6 inductively coupled plasma (ICP) spectrometer (BAIRD, American).

3. Results and discussion

3.1. X-ray diffraction

Fig. 1 shows the XRD patterns of $Li_{1-x}Na_xFePO_4/C$ (x = 0, 0.01, 0.03, 0.05) samples. The crystal phases of all the samples were to be an ordered olivine structure indexed by orthorhombic *Pnma*, and no other impurities were detected. There was no evidence for the formation of crystalline or amorphous carbons. This was undoubtedly because the content of the residual carbon was about 3.8 wt.%, determined by element analysis. It was obvious that doping a low amount of Na did not affect the structure of the samples. The doping of Na would be inclined to occupy Li sites because the phase of $NaFePO_4$ was structurally analogous to $LiFePO_4$ [17,18] and that Na and Li atoms had the same outer electronic structure. Table 1 shows the cell parameters of the samples calculated by XRD analysis. As can be seen, the lattice parameters changed slightly with the increasing amount of Na, which was in agreement with the fact that Na ion (r = 0.97 Å) had larger radius than that of Li ion (r = 0.68 Å) in octahedral coordination. However, when the doping amount is too high, perhaps the structure of the formed $LiFePO_4$ will be different, and unfavourable results will appear [19]. The values a, c, and v of the $Li_{0.97}Na_{0.03}FePO_4/C$ sample were the largest among all the prepared powders, indicating the doped one had the widest Li ion pathway [15]. While decrease of the lattice parameter b would shorten the diffusion distance of Li ion and enhance the Li^+ intercalation/de-intercalation [20].

3.2. SEM and TEM morphology

Fig. 2 shows SEM images of $LiFePO_4/C$ (Fig. 2(a)) and $Li_{0.97}Na_{0.03}FePO_4/C$ (Fig. 2(b)). It can be seen clearly that the particle was a kind of secondary particle composed of small size particles.

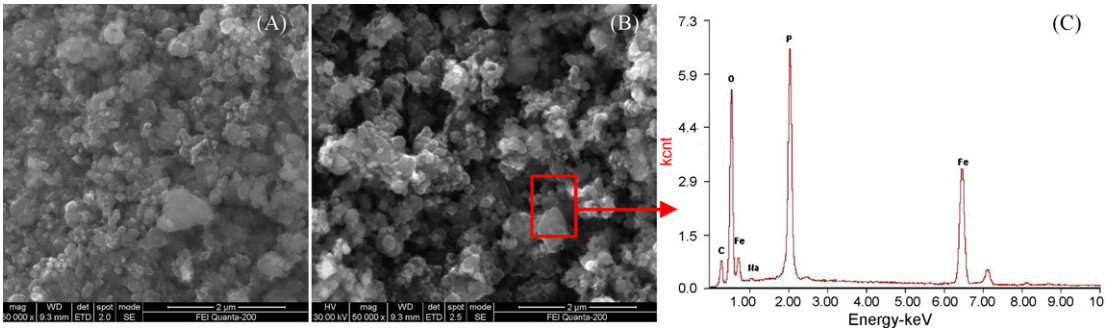

Fig. 2. SEM images of $LiFePO_4/C$ (a) and $Li_{0.97}Na_{0.03}FePO_4/C$ (b) with corresponding EDAX map (c).

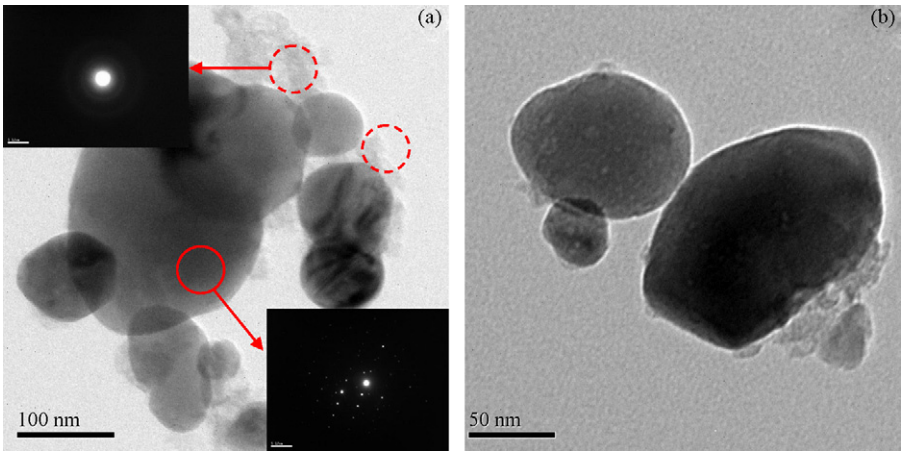

Fig. 3. TEM images of $Li_{0.97}Na_{0.03}FePO_4/C$, and the insets are SAED patterns of the bulk region and particle boundary, respective.

The average particle sizes of two samples were around 100 nm with sphere-like morphology. The reduction of particle size could be attributed to in situ restrictive methods which interfered with the growth of the grains. The EDS result of $Li_{0.97}Na_{0.03}FePO_4/C$ (Fig. 2(c)) unambiguously confirmed that the particles in the selected region included Fe, P, O, and C components with a trace of Na, which were in accord with above analysis.

The TEM images of $Li_{0.97}Na_{0.03}FePO_4/C$ are shown in Fig. 3. Inserts in Fig. 3 exhibit selected area diffraction patterns for the particles and web, which indicate that the particle is crystalline $LiFePO_4$ and the web is an amorphous carbon. Obviously, nano-carbons (marked with dashed circle) were wrapping and connecting particles to build the web structure. Besides, we found that some of particles were bonded together by carbon network which was generated by carbonization of the PANI shell and glucose precursor. During the heat treatment process, the polymer shell was transformed into carbon shell that restricted the in situ crystallite growth of $LiFePO_4$. The $LiFePO_4$ crystallites with a carbon shell connected together, thereby further ensured electrical continuity around the crystallites.

3.3. Electrochemical measurements

The initial charge/discharge curves of the $Li_{1-x}Na_xFePO_4/C$ samples at 0.1 C rate between cutoff voltage 2.5 and 4.2 V are shown in Fig. 4(a). The initial special discharge capacities for $Li_{1-x}Na_xFePO_4/C$ samples with $x = 0$, 0.01, 0.03, and 0.05 were 151, 154, 158, and 148 mAh g^{-1}, respectively. As the Na content increased to 0.05, the first irreversible capacities became smaller due to the decreasing lithium content. For comparison, the results of capacity retention study cycled at 1 C are plotted in Fig. 4(b). It can be seen that improvement in discharge capability and cycle performance was realized by appropriate amount of Na doping. Among the prepared $Li_{1-x}Na_xFePO_4/C$ ($0 \le x \le 0.05$) powders, $Li_{0.97}Na_{0.03}FePO_4/C$ sample exhibited the best electrochemical performance. Initial discharge capability and cycle performance of $Li_{0.97}Na_{0.03}FePO_4/C$ electrodes at various rates are displayed in Fig. 5. The $Li_{0.97}Na_{0.03}FePO_4/C$ sample exhibited discharge capacity of 158, 151, 142, 134, and 105 mAh g^{-1} as it was discharged at 0.1, 0.5, 1, 2, and 3 C, respectively.

It is obvious that the sample doped by appropriate amount of Na ion exhibits better electrochemical properties, which can be interpreted as the enhancement of electronic and ionic conductivity by ion doping. Based on the first-principles calculations, Ouyang et al. [15] concluded that both the electronic conductive properties and the ionic transport feature were improved by Na doping, compared with the high valance metal ions doping and pure $LiFePO_4$. The fact that the decreasing migration energy barriers for Li ions in the Na-doped $LiFePO_4$ indicated that the Na ions at Li sites would not block the Li ions diffusion similarly to high valence transition metal ions. The increased ionic conductivity was ascribed to the expanded diffusion pathway and the decreased Li–O interaction. Meanwhile, it was found that the insertion and extraction of Na ion was hardly

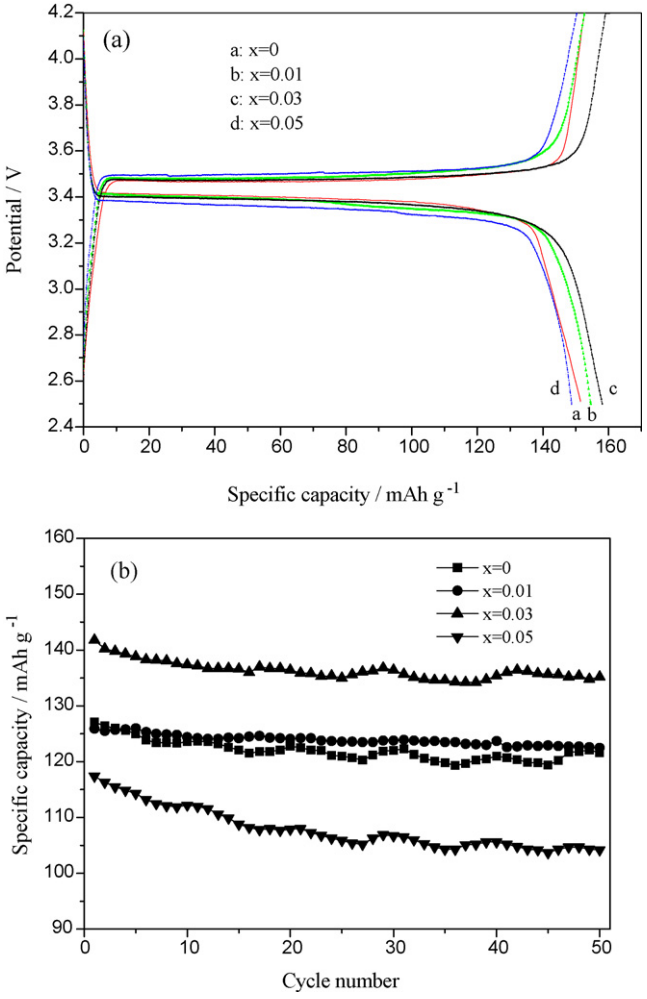

Fig. 4. Initial charge and discharge curves of $Li_{1-x}Na_xFePO_4/C$ ($0 \le x \le 0.05$) electrodes at 0.1 C (a) and cycle performance of electrodes at 1 C (b).

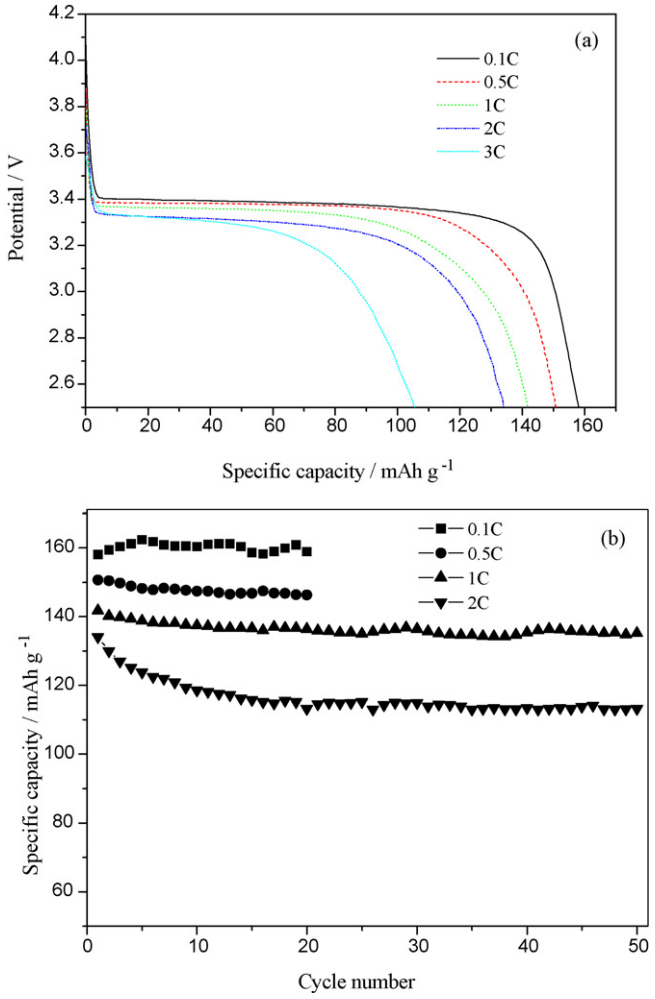

Fig. 5. Initial discharge curves (a) and cycle performance (b) of $Li_{0.97}Na_{0.03}FePO_4/C$ electrodes at various rates.

taken place during the charge and discharge process, because the ICP measurements showed that the concentration of Na ion in the electrolyte of the cells after 10 cycles of charge and discharge was so low that it cannot be detected. These results suggested that the Na ions might be played a pillar in structure. Park et al. [21] reported that the structure of $Li_{1.1-x}Na_xNi_{0.2}Co_{0.3}Mn_{0.4}O_2$ was stabilized by incorporating Na ion. This kind of pillar effect provided larger space for the movement of lithium ions [19,25]. Consequently, the conductivity was enhanced and the lithium ion diffusion coefficient was boosted after doping. Furthermore, the improvement of electronic conductivity by Na doping had been verified by four-point probe method. All doped compositions had the electronic conductivity of the order of 10^{-2} S cm^{-1} at room temperature. The electronic conductivity of $Li_{0.97}Na_{0.03}FePO_4/C$ and undoped $LiFePO_4/C$ were 1.9×10^{-2} and 5.54×10^{-3} S cm^{-1}, respectively. The results indicate that the sodium doped sample certainly obtains larger electronic conductivity which may be attributed to the aberrance of the crystal structure introduced by the doped Na ions in the crystal. The explicit mechanism remains to be further studied.

Cyclic voltammetry measurements were performed on $Li_{1-x}Na_xFePO_4/C$ electrodes to identify the characteristics of the redox reactions in Li-ion cells as shown in Fig. 6. A couple of redox current peaks appeared on each voltammogram curve. Among them, the $Li_{0.97}Na_{0.03}FePO_4/C$ sample showed the best electrochemical behavior, with the highest peak current and the narrowest potential margin between the anodic current peak

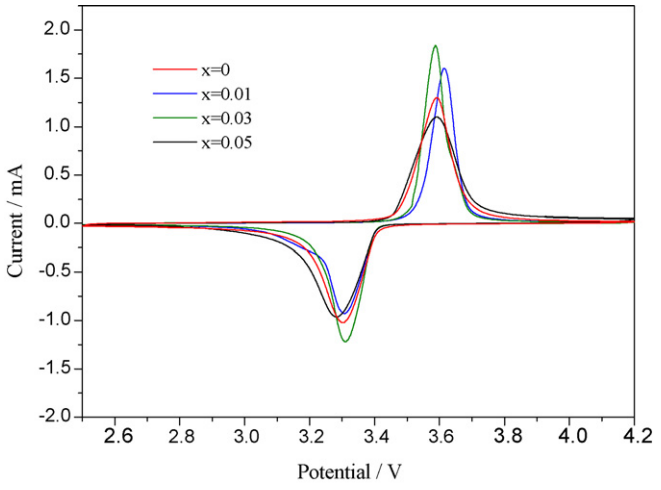

Fig. 6. Cyclic voltammograms of lithium cells with $Li_{1-x}Na_xFePO_4/C$ composite, the second cycle at a scanning rate of 0.1 mV s^{-1}.

(3.58 V) and the cathodic current peak (3.31 V). In the case of the $LiFePO_4/C$, the potential separation between anodic and cathodic peaks is 0.29 V. As for cyclic voltammogram, the potential interval between anodic peak and cathodic peak is an important parameter to evaluate the electrochemical reaction reversibility. The well-defined peaks and narrower peak separation suggested that the reversibility of the electrode reaction was improved by Na doping.

EIS was applied to further analyze the effect of Na doping on electrode impedance. Before EIS tests, all the half-cells were charged to 3.4 V at the second cycle and equilibrated at 3.4 V. Fig. 7(a) represents the Nyquist plots of $LiFePO_4/C$ and $Li_{0.97}Na_{0.03}FePO_4/C$ samples at ambient temperature. In Fig. 7(a), the impedance spectra curves were composed of a depressed semicircle in high frequency region and a straight line in low frequency region. An intercept at the Z_{re} axis at high frequency corresponded to the ohmic resistance (R_e), which represented the resistance of the electrolyte and electrode. The semicircle in the middle frequency range indicated the charge transfer resistance (R_{ct}). The inclined line in the low frequency range represented the Warburg impedance (Z_w), which was associated with lithium-ion diffu-

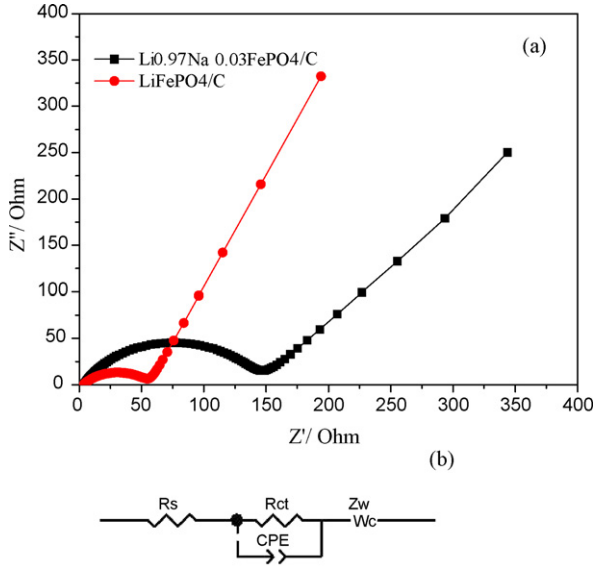

Fig. 7. EIS spectra of $LiFePO_4/C$ and $Li_{0.97}Na_{0.03}FePO_4/C$ cathodes (a) and equivalent circuit (b).

sion in $LiFePO_4$ particles. A simplified equivalent circuit model (Fig. 7(b)) was constructed to analyze the impedance spectra. A constant phase element CPE was placed to represent the double layer capacitance and passivation film capacitance. The charge transfer resistances (R_{ct}) of $LiFePO_4$/C and $Li_{0.97}Na_{0.03}FePO_4$/C composite were 139.6 and 53.0 Ω, respectively. The charge transfer resistance is related to complex reaction process of charge transfer between the electrolyte and the active materials [23,24]. The smaller resistance indicates that Li ion and electron transfer are more feasible on the electrode, which may be attributed to the decreasing electric resistance of the composite material measured by four-point probe method [26]. Therefore, the electric resistance of the composite cathode was reduced by doping of a certain amount of Na^+, indicating that doping metal ion is an effective way to improve the electrochemical activity of $LiFePO_4$/C [7,22].

4. Conclusions

Olivine structured $Li_{1-x}Na_xFePO_4$/C (x = 0, 0.01, 0.03, 0.05) samples were synthesized by in situ polymerization restriction–carbonthermal reduction method. XRD analysis showed that no other impurities were detected and that the lattice parameters changed with the amount of Na^+ doping. The $Li_{0.97}Na_{0.03}FePO_4$/C sample showed the highest reversible capacity and improved rate capability, which might be attributed to its larger lattice parameters in a and c than those of other samples prepared in this study. The $Li_{0.97}Na_{0.03}FePO_4$/C sample exhibited initial discharge capacity of 158, 151, 142, 134, and 105 mAh g^{-1} as it was discharged with 0.1, 0.5, 1, 2, and 3 C rates, respectively. The modified electrochemical performance, proved by CV and EIS tests, indicated that Na ion doping would help to improve the electrochemical activity of $LiFePO_4$/C.

Acknowledgement

This work was financially supported by Chinese 863 program (No. 2008AA031205).

References

[1] A.K. Padhi, K.S. Nanjundaswamy, J.B. Goodenough, J. Electrochem. Soc. 144 (1997) 1188.
[2] M. Yonemura, A. Yamada, Y. Takei, N. Sonoyama, R. Kanno, J. Electrochem. Soc. 151 (2004) A1352.
[3] S.Y. Chung, J.T. Bloking, Y.M. Chiang, Nat. Mater. 1 (2002) 123.
[4] C. Delacourt, P. Poizot, J.M. Tarascon, C. Masquelier, Nat. Mater. 4 (2005) 254.
[5] C.R. Sides, F. Croce, V.Y. Young, C.R. Martin, B. Scrosati, Electrochem. Solid-State Lett. 8 (2005) A484.
[6] K.S. Parka, J.T. Sona, H.T. Chung, S.J. Kim, C.H. Lee, K.T. Kang, H.G. Kim, Solid State Commun. 129 (2004) 311.
[7] C.H. Mi, Y.X. Cao, X.G. Zhang, X.B. Zhao, H.L. Li, Powder Technol. 181 (2008) 301.
[8] Y.S. Hu, Y.G. Guo, R. Dominko, M. Gaberscek, J. Jamnik, J. Maie, Adv. Mater. 19 (2007) 1963.
[9] C. Delacourt, P. Poizot, S. Levasseur, C. Masquelier, Electrochem. Solid-State Lett. 9 (2006) A352.
[10] D. Choi, P.N. Kumta, J. Power Sources 163 (2007) 1064.
[11] P.S. Herle, B. Ellis, N. Coombs, L.F. Nazar, Nat. Mater. 3 (2004) 147.
[12] C.Y. Ouyang, S.Q. Shi, Z.X. Wang, H. Li, X.J. Huang, L.Q. Chen, Phys. Rev. B 69 (2004) 1.
[13] D. Morgan, A. Van der Ven, G. Ceder, Electrochem. Solid-State Lett. 7 (2004) A30.
[14] C.Y. Ouyang, S.Q. Shi, Z.X. Wang, H. Li, X.J. Huang, L.Q. Chen, J. Phys: Condens. Matter 16 (2004) 2265.
[15] C.Y. Ouyang, D.Y. Wang, S.Q. Shi, Z.X. Wang, H. Li, X.J. Huang, L.Q. Chen, Chin. Phys. Lett. 23 (2006) 61.
[16] Y.G. Wang, Y.R. Wang, E. Hosono, K.X. Wang, H.S. Zhou, Angew. Chem. Int. Ed. 47 (2008) 7461.
[17] O.V. Yakubovich, E.L. Belokoneva, V.G. Tsirel'son, V.S. Urusov, Vestn. Mosk. Univ. Ser. 4: Geol. 6 (1992) 54.
[18] J.N. Birdson, S.E. Quinlan, P.R. Tremaine, Chem. Mater. 10 (1998) 763.
[19] H. Liu, Q. Cao, L.J. Fu, C. Li, Y.P. Wu, H.Q. Wu, Electrochem. Commun. 8 (2006) 1553.
[20] L.Q. Sun, R.H. Cui, A.F. Jalbout, M.J. Li, X.M. Pan, R.S. Wang, H.M. Xie, J. Power Sources 189 (2009) 522.
[21] S.H. Park, S.S. Shin, Y.K. Sun, Mater. Chem. Phys. 95 (2006) 218.
[22] F. Gao, Z.Y. Tang, Electrochim. Acta 53 (2008) 5071.
[23] J.L. Liu, R.R. Jiang, X.Y. Wang, T. Huang, A.S. Yu, J. Power Sources 194 (2009) 536.
[24] J. Molenda, W. Ojczyk, J. Marzec, J. Power Sources 174 (2007) 689.
[25] P.K. Sharma, G.J. Moore, F. Zhang, P. Zavalij, M.S. Whittingham, Electrochem. Solid-State Lett. 2 (1999) 494.
[26] D. Aurbach, M.D. Levi, E. Levi, H. Teller, B. Markovsky, G. Salitra, U. Heider, L. Heider, J. Electrochem. Soc. 145 (1998) 3024.